Robust Fitting by Adaptive-Scale Residual Consensus

Hanzi Wang and David Suter

Department of Electrical and Computer Systems Engineering
Monash University, Clayton Vic. 3800, Australia
{hanzi.wang,d.suter}@eng.monash.edu.au

Abstract. Computer vision tasks often require the robust fit of a model to some data. In a robust fit, two major steps should be taken: i) robustly estimate the parameters of a model, and ii) differentiate inliers from outliers. We propose a new estimator called Adaptive-Scale Residual Consensus (ASRC). ASRC scores a model based on both the residuals of inliers and the corresponding scale estimate determined by those inliers. ASRC is very robust to multiple-structural data containing a high percentage of outliers. Compared with RANSAC, ASRC requires no pre-determined inlier threshold as it can simultaneously estimate the parameters of a model and the scale of inliers belonging to that model. Experiments show that ASRC has better robustness to heavily corrupted data than other robust methods. Our experiments address two important computer vision tasks: range image segmentation and fundamental matrix calculation. However, the range of potential applications is much broader than these.

1 Introduction

Unavoidably, computer vision data is contaminated (e.g., faulty feature extraction, sensor noise, segmentation errors, etc) and it is also likely that the data include multiple structures. Considering any particular structure, outliers to that structure can be classified into gross outliers and pseudo outliers [16], the latter being data belonging to other structures. Computer vision algorithms should be robust to outliers including pseudo outliers [6]. Robust methods have been applied to a wide variety of tasks such as optical flow calculation [1, 22], range image segmentation [24, 15, 11, 10, 21], estimating the fundamental matrix [25, 17, 18], etc.

The breakdown point is the smallest percentage of outliers that can cause the estimator to produce arbitrarily large values ([13], pp.9.). Least Squares (LS) has a breakdown point of 0%. To improve on LS, robust estimators have been adopted from the statistics literature (such as M-estimators [9], LMedS and LTS [13], etc) but they tolerate no more than 50% outliers, limiting their suitability [21]. The computer vision community has also developed techniques to cope with outliers: e.g., the Hough Transform [8], RANSAC [5], RESC [24], MINPRAN [15], MUSE [11], ALKS [10], pbM-estimator [2], MSAC and MLESAC [17]. The Hough Transform determines consensus for a fit from "votes" in a binned parameter space: however one must choose the bin size wisely and, in any case, this technique suffers from high cost when the number of parameters is large. Moreover, unlike the other techniques, it returns a limited precision result (limited by the bin size). RANSAC requires a user-

T. Pajdla and J. Matas (Eds.): ECCV 2004, LNCS 3023, pp. 107–118, 2004.

supplied error tolerance. RESC attempts to estimate the residual probability density function but the method needs the user to tune many parameters and we have found that it overestimates the scale of inliers. MINPRAN assumes that the outliers are randomly distributed within a certain range, making MINPRAN less effective in extracting multiple structures. MUSE requires a lookup table for the scale estimator correction and ALKS is limited in its ability to handle extreme outliers.

In this paper, we propose (section 0) a new robust estimator: Adaptive-Scale Residual Consensus (ASRC), which is based on a robust two-step scale estimator (TSSE) (section 0). We apply ASRC to range image segmentation and fundamental matrix calculation (section 0) demonstrating that ASRC outperforms other methods.

2 A Robust Scale Estimator: TSSE

TSSE [23] is derived from kernel density estimation techniques and the mean shift/mean shift valley method. Kernel estimation is a popular method for probability density estimation [14]. For n data points $\{X_i\}_{i=1,\dots,n}$ in a 1-dimensional residual space, the kernel density estimator with kernel K and bandwidth h is ([14], p.76):

$$\hat{f}(x) = \frac{1}{nh}\sum_{i=1}^{n} K\left(\frac{x - X_i}{h}\right) \tag{1}$$

The Epanechnikov kernel ([14], p.76)

$$K(X) = \frac{3}{4}(1 - X^2) \quad if\ (1 - X^2) > 0;\ 0 \quad otherwise \tag{2}$$

is optimum in terms of minimum mean integrated square error (MISE), satisfying various conditions ([19], p.95). Using such a kernel, the mean shift vector $\mathrm{M_h}(x)$ is:

$$\mathrm{M_h}(x) \equiv \frac{1}{n_x}\ {}_{X_i \in S_h(x)}(X_i - x) = \frac{1}{n_x}\ {}_{X_i \in S_h(x)} X_i - x \tag{3}$$

where $S_h(x)$ is a hypersphere of the radius h, having the volume $h^d c_d$ (c_d is the volume of the unit d-dimensional sphere, e.g., c_1=2), centered at x, and containing n_x data points.

Marching in the direction of this vector we perform gradient ascent to the peak. However, for TSSE we also need to find the valleys. Based upon the Gaussian kernel, a saddle-point seeking method was published in [4] but we employ a more simple method [20], based upon the Epanechnikov kernel and, for our purposes, in 1-D residual space. The basic idea is to define the mean shift valley vector as:

$$\mathrm{MV_h}(x) = \text{-}\mathrm{M_h}(x) = x - \frac{1}{n_x}\sum_{X_i \in S_h(x)} X_i \tag{4}$$

In order to avoiding the oscillations, we modify the step size as follows. Let $\{y_i\}_{i=1,2\dots}$ be the sequence of successive locations of the mean shift valley procedure, then we have, for each i=1,2…,

$$\mathrm{y}_{i+1} = y_i + \tau \cdot MV_h(y_i) \tag{5}$$

where τ is a correction factor, and 0<τ ≤1. If the shift step at y_i is too large, it causes y_{i+1} to jump over the local valley and thus oscillate over the valley. This problem can be avoided by adjusting τ so that $MV_h(y_i)^T MV_h(y_{i+1})>0$.

A crucial issue in implementing the TSSE is the kernel bandwidth choice [19, 3]. A simple over-smoothed bandwidth selector can be employed [19].

$$\hat{h}=\left[\frac{243R(K)}{35u_2(K)^2 n}\right]^{1/5} S \tag{6}$$

where $R(K)=\int_{-1}^{1} K(\zeta)^2 d\zeta$ and $u_2(K)=\int_{-1}^{1}\zeta^2 K(\zeta)d\zeta$. S is the sample standard deviation.

The median [13], MAD [12] or robust k [10] scale estimator can be used to yield an initial scale estimate. It is recommended that the bandwidth be set as $c\hat{h}$, (0<c<1) to avoid over-smoothing ([19], p.62).

We can now describe the TSSE process:

1. Use mean shift, with initial center zero, to find the local peak, and then we use the mean shift valley to find the valley next to the peak: all in ascending ordered absolute residual space.
2. Estimate the scale of the fit by the median scale estimator [13] on the points whose residuals are within the obtained band centered at the local peak.

Based on TSSE, a new robust estimator (ASRC) will be provided in the next section.

3 Robust Adaptive-Scale Residual Consensus Estimator

We assume that when a model is correctly found, two criteria should be satisfied:

- The (weighted) sum of absolute residuals (r_i) of the inliers should be small.
- The scale (S) (standard variance) of the inliers should be small.

Given S, the inliers are those that satisfy:

$$\left| r_{\vartheta i}/S_{\vartheta} \right| < T \tag{7}$$

where T is a threshold. If T is 2.5(1.96), then 98%(95%) percent of a Gaussian distribution will be identified as inliers. In our experiments, T=2.5 (except for section 0 where T=1.96)

$$\hat{\theta}=\arg\max_{\hat{\theta}}\left(\frac{\sum_{i=1}^{n_{\hat{\theta}in}}\left(1-\left|r_{\hat{\theta}i}/(S_{\hat{\theta}}T)\right|\right)}{S_{\hat{\theta}}}\right) \tag{8}$$

where $n_{\hat{\theta}in}$ is the number of inliers which satisfies equation (7) for the fitted $\hat{\theta}$.

No priori knowledge about the scale of inliers is necessary as the proposed method yields the estimated parameters of a model and the corresponding scale simultaneously.

The ASRC estimator algorithm is as follows (for fitting models with p parameters):

1. Randomly choose one p-subset from the data points, estimate the model parameters using the p-subset, and calculate the ordered absolute residuals.

2. Choose the bandwidth by equation (6). A robust *k* scale estimator [10] (*k*=0.2) is used to yield a coarse initial scale S_0.
3. Apply TSSE to the absolute sorted residuals to estimate the scale of inliers S_1. Because the robust *k* scale estimator is biased for data with multiple structures, use S_1 in equation (6) to apply TSSE again for the final scale of inliers S_2.
4. Validate the valley. The probability density at the local peak $\hat{f}(peak)$ and local valley $\hat{f}(valley)$ are obtained by equation (1). Let $\hat{f}(valley)/\hat{f}(peak)=\lambda$ (where $1>\lambda\geq 0$). Because the inliers are assumed having a Gaussian-like distribution, the valley is not sufficiently deep when λ is too large (say, larger than 0.8). If the valley is sufficiently deep, go to step (5); otherwise go to step (1).
5. Calculate the score, i.e., the objective function of the ASRC estimator.
6. Repeat step (1) to step (5) *m* times. Finally, output the parameters and the scale S_2 with the highest score.

Let ε be the fraction of outliers, *P* the probability that at least one of the *m* *p*-tuples is "clean"; then one can determine *m* by ([13], pp.198):

$$m=\frac{\log(1-P)}{\log[1-(1\text{-}\varepsilon)^p]} \tag{9}$$

In [23], we propose a robust Adaptive Scale Sample Consensus (ASSC) estimator:

$$\hat{\theta}=\arg\max_{\hat{\theta}}(n_{\hat{\theta}in}/S_{\hat{\theta}}) \tag{10}$$

From equation (8) and (10), we can see that the difference between ASRC and our recently proposed ASSC [23] is: in ASSC, all inliers are treated as the same, i.e., each inlier contributes 1 to the object function of ASSC. However, in ASRC, the sizes of the residuals of inliers are influential.

4 Experiments

4.1 Synthetic Examples on Line Fitting and Plane Fitting

The proposed method is compared with LMedS, RESC, ALKS, and our recently proposed method: ASSC. We generated four examples: roof, 'F'-figure, one-step, and three-step linear signals (the signals are in the magenta color), each with a total of 500 data points, corrupted by Gaussian noise with zero mean and standard variance σ. Among the 500 data points, α data points were randomly distributed in the range of (0, 100). The *i*'th structure has n_i data points: **(a)** Roof: x:(0-50), y=2x, n_1=65; x:(50-100), y=200-2x, n_2=50; α=385; σ=1. **(b)** F-figure: x:(25-75), y=85, n_1=40; x:(25-75), y=70, n_2=35; x=25, y:(30-85), n_3=35; α=390; σ=1.2. **(c)** Step: x:(0-50), y=75, n_1=45; x:(50-100), y=60, n_2=45; α=410; σ=1. **(d)** Three-step: x:(0-25), y=20, n_1=45; x:(25-50), y=40, n_2=30; x:(50-75), y=60, n_3=30; x:(75-100), y=80, n_4=30; α=365; σ=1.

From Fig. 1 we can see that ASRC correctly fits all four signals. LMedS (50% breakdown point) failed to fit all four. Although ALKS is sometimes more robust, it also failed. RESC and ASSC succeeded in the roof signal (87% outliers), however, they both failed in the other three cases. It should be emphasized that both the

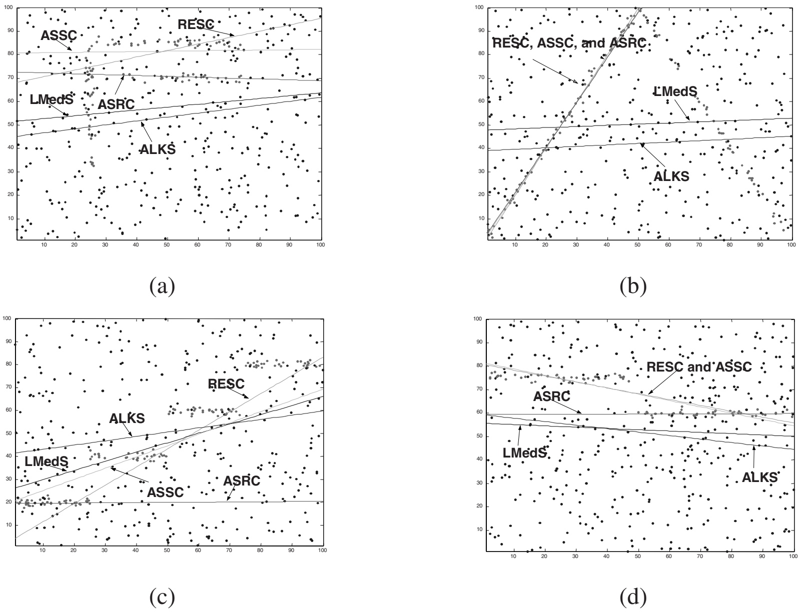

Fig. 1. Comparing the performance of five methods: (a) fitting a roof with a total of 87% outliers; (b) fitting F-figure with a total of 92% outliers; (c) fitting a step with a total of 91% outliers; (d) fitting three-step with a total of 91% outliers.

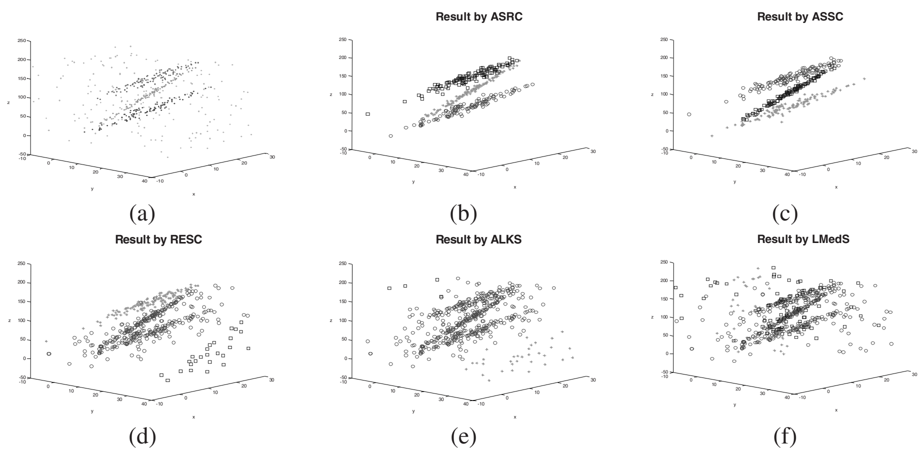

Fig. 2. (a) the 3D data with 80% outliers; the extracted results by (b) ASRC; (c) ASSC; (d) RESC; (e) ALKS; and (f) LMedS.

bandwidth choice and the scale estimation in ASRC are data-driven: an improvement over RANSAC where the user sets a priori scale-related error bound.

Next, two 3D signals were used: 500 data points and three planar structures with each plane containing n points corrupted by Gaussian noise with standard variance σ (=3.0); 500-3n points are randomly distributed. In the first example, n =100; in the second $n = 65$. We repeat: (1) estimate the parameters and scale of a plane (2) extract the inliers and remove them from the data set - until all planes are extracted. The red circles denote the first plane extracted; green stars the second; and blue squares the third (Fig. 2 and Fig. 3).

From Fig. 2 (d) and (e), we can see that RESC and ALKS, which claim to be robust to data with more than 50% outliers, failed to extract all the three planes. This is because the estimated scales (by RESC and ALKS) for the first plane were wrong, which caused these two methods to fail to fit the second and third planes. Because the LMedS (in Fig. 2 (d)) has only a 50% breakdown point, it completely failed to fit data with such high contamination — 80% outliers. The proposed method and ASSC yielded the best results (Fig. 2 (b) and (c)). Similarly, in the second 3D experiment (Fig. 3), RESC, ALKS and LMedS completely broke down. ASSC, although it correctly fitted the first plane, wrongly fitted the second and the third planes. Only the proposed method correctly fitted and extracted all three planes (Fig. 3 (b)).

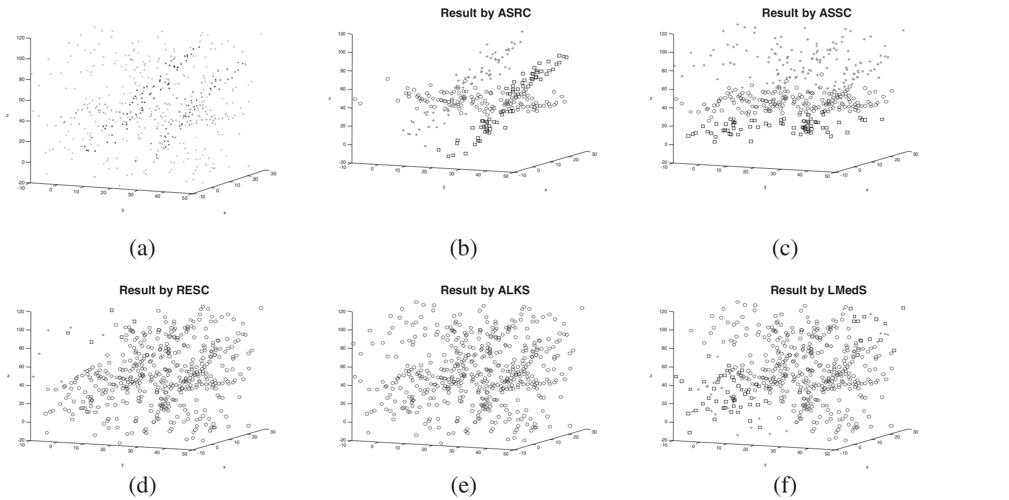

Fig. 3. (a) the 3D data with 87% outliers; the extracted results by (b) ASRC; (c) ASSC; (d) RESC; (e) ALKS; and (f) LMedS.

4.2 Range Image Segmentation

Many robust estimators have been employed to segment range images ([24, 11, 10, 21], etc.). Here, we use the ABW range images (obtained from http://marathon.csee.usf.edu/seg-comp/SegComp.html.) The images have 512x512 pixels and contain planar structures. We employ a hierarchal approach with four levels [21]. The bottom level of the hierarchy contains 64x64 pixels that are obtained by using regular sampling on the original image. The top level of the hierarchy is the original image. We begin with bottom level. In each level of the hierarchy, we:

(1) Apply the ASRC estimator to obtain the parameters of plane and the scale of inliers. If the number of inliers is less than a threshold, go to step (6).
(2) Use the normals to the planes to validate the inliers obtained in step (1). When the angle between the normal of the data point that has been classified as an

inlier, and the normal of the estimated plane, is less than a threshold value, the data point is accepted. Otherwise, the data point is rejected and will be left for further processing. If the number of the validated inliers is small, go to step (6).

(3) Fill in the holes, which may appear due to sensor noise, inside the maximum connected component (CC) from the validated inliers.

(4) In the top hierarchy, assign a label to the points corresponding to the CC from step (3) and remove these points from the data set.

(5) If a point is unlabelled and it is not a jump edge point, the point is a "left-over" point. After collecting all these, use the CC algorithm to get the maximum CC. If the number data points of the maximum CC of "left-over" points is smaller than a threshold, go to step (6); otherwise, sample the maximum CC obtained in this step, then go to step (1).

(6) Terminate the processing in the current level of the hierarchy and go to the higher-level hierarchy until the top of the hierarchy.

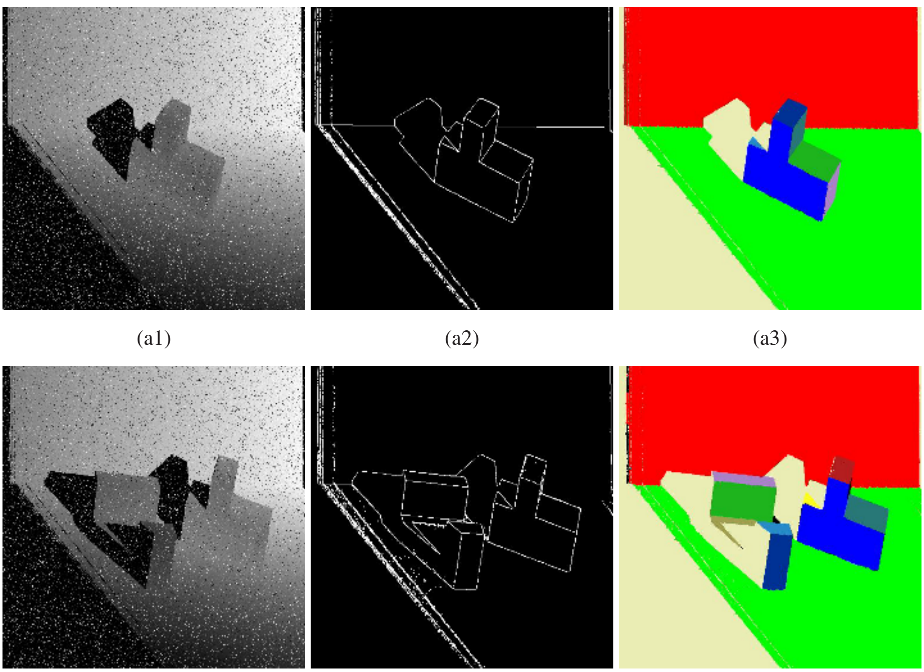

(a1) (a2) (a3)

(b1) (b2) (b3)

Fig. 4. Segmentation of ABW range images from the USF database. (a1, b1) Range image with 26214 random noise points; (a2, b2) The ground truth results for the corresponding range images without adding random noise; (a3, b3) Segmentation result by ASRC.

The proposed range image segmentation method is very robust to noise. We added 26214 random noise points to the range images (in Fig. 4) taken from the USF ABW range image database ("test 11" and "test 3"). No separate noise filtering is performed. All of the main surfaces were recovered by our method.

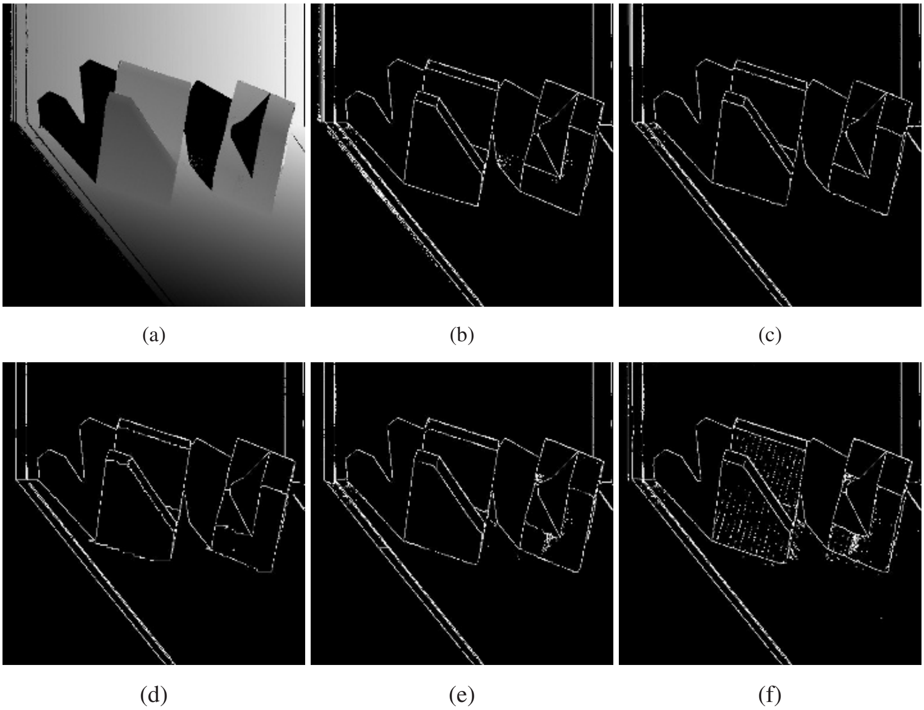

Fig. 5. Comparison of the segmentation results for ABW range image (train 7). (a) Range image; (b) The result of ground truth; (c) The result by the ASRC; (d) The result by the UB; (e) The result by the WSU; (f) The result by the USF.

We also compared our results with those of three state-of-the-art approaches of USF, WSU, and UB [7]. Fig. 5 (c-f), showing the results obtained by the four methods should be compared with the results of the ground truth (Fig. 5 (b)).

From Fig. 5, we can see that the proposed method achieved the best results: all surfaces are recovered and the segmented surfaces are relatively "clean". In comparison, some boundaries on the junction of the segmented patch by the UB were seriously distorted. The WSU and USF results contained many noisy points and WSU over segmented one surface. The proposed method takes about 1-2 minutes (on an AMD800MHz personal computer in C interfaced with MATLAB language).

4.3 Fundamental Matrix Estimation

Several robust estimators, such as M-estimators, LMedS, RANSAC, MSAC and MLESAC, have been applied in estimating the fundamental matrix [17]. However, M-estimators and the LMedS have a low breakdown point, RANSAC and MSAC need a- priori knowledge about the scale of inliers. MLESAC performs similar to MSAC.

The proposed ASRC can tolerate more than 50% outliers; and no priori scale information about inliers is required.

Let $\{x_{i,}\}$ and $\{x_i'\}$ (for i=1,…,n) to be a set of homogeneous image points viewed in image 1 and image 2. We have the following constraints for the fundamental matrix F:

$$x_i^{'T} F x_i = 0 \; and \; \det[F] = 0 \tag{11}$$

We employ the 7 points algorithm [17] to solve for candidate fits using Simpson distance - for the i'th correspondence r_i using Simpson distance is:

$$r_i = \frac{k_i}{\left(k_x^2 + k_y^2 + k_{x'}^2 + k_{y'}^2\right)^{1/2}} \tag{12}$$

$$where\; k_i = f_1 x_i^{'} x_i + f_2 x_i^{'} y_i + f_3 x_i^{'} \varsigma + f_4 y_i^{'} x_i + f_5 y_i^{'} y_i + f_6 y_i^{'} \varsigma + f_7 x_i \varsigma + f_8 y_i \varsigma + f_9 \varsigma^2 .$$

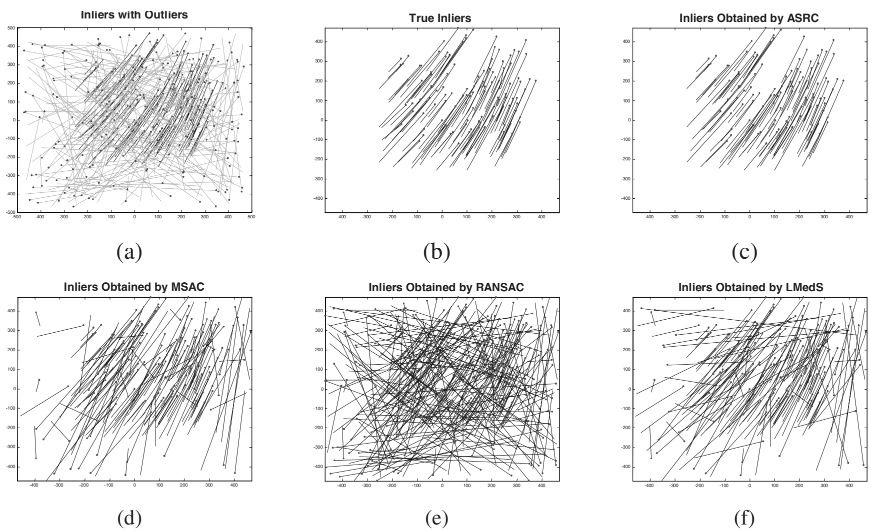

Fig. 6. An experimental comparison of estimating fundamental matrix for data with 60% outliers. (a) The distributions of inliers and outliers; (b) The distribution of true inliers; The inliers obtained by (c) ASRC; (d) MSAC; (e) RANSAC; and (f) LMedS.

Table 1. An experimental comparison for data with 60% outliers.

	% of inliers correctly classified	% of outliers correctly classified	Standard variance of inliers
Ground Truth	100.00	100.00	0.9025
ASRC	95.83	100.00	0.8733
MSAC	100.00	65.56	41.5841
RANSAC	100.00	0.56	206.4936
LMedS	100.00	60.00	81.1679

We generated 300 matches including 120 point pairs of inliers with unit Gaussian variance (matches in blue color in Fig. 6(a)) and 160 point pairs of random outliers (matches in cyan color in Fig. 6(a)). Thus the outliers occupy 60% of the whole data.

The scale information about inliers is usually not available, thus, the median scale estimator, as recommended in [17], is used for RANSAC and MSAC to yield an initial scale estimate. The number of random samples is set to 10000. From Fig. 6 and Table 1, we can see that our method yields the best result.

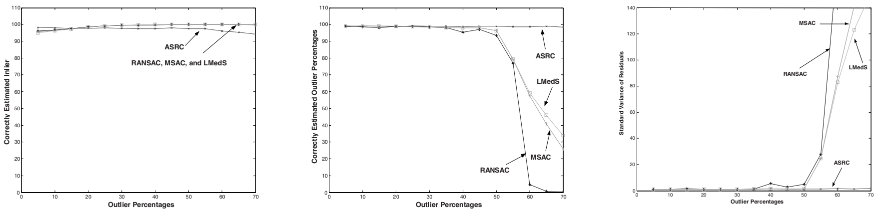

(a) (b) (c)

Fig. 7. A comparison of correctly identified percentage of inliers (a), outliers (b), and the comparison of standard variance of residuals of inliers (c).

Table 2. Experimental results on two frames of the Corridor sequence.

	Number of inliers	Mean error of inliers	Standard variance of inliers
ASRC	269	–0.0233	0.3676
MSAC	567	–0.9132	7.5134
RANSAC	571	–1.2034	8.0816
LMedS	571	–1.1226	8.3915

Next, we investigate the behavior for data involving different percentages of outliers (PO). We generated the data (in total 300 correspondences) similar to that in Fig. 6. The percentage of outliers varies from 5% to 70% in increments of 5%. The experiments were repeated 100 times for each percentage of outliers. If a method is robust enough, it should resist the influence of outliers and the correctly identified percentages of inliers should be around 95% (T is set 1.96 in equation (7)) and the standard variance of inliers should be near to 1.0 despite of the percentages of outliers.

We set the number of random samples, m, to be: m =1000 when PO≤40; 10000 when 40<PO≤60; and 30000 when PO>60 to ensure a high probability of success.

From Fig. 7, we can see that MSAC, RANSAC, and LMedS all break down when data involve more than 50% outliers. The standard variance of inliers by ASRC is the smallest when PO >50%. Note: ASRC succeeds to find the inliers and outliers even when outliers occupied 70% of the whole data.

Next, two frames of the Corridor sequence (bt.000 and bt.004), were obtained from http://www.robots.ox.ac.uk/~vgg/data/ (Fig. 8(a) and (b)). Fig. 8(c) shows the matches involving 800 point pairs in total. The inliers (269 correspondences) obtained by the proposed method are shown in Fig. 8(d). The epipolar lines and epipole using the estimated fundamental matrix by ASRC are shown in Fig. 8(e) and (f). In Fig. 8(e) and (f), we draw 30 epipolar lines. We can see that most of the point pairs correspond to the same feature in the two images except for one case: the 30th point pair, which is pointed out by the two arrows. The reason is that the residual of the point pair corresponding to the estimated fundamental matrix is small: the epipolar constraint is a weak constraint and ANY method enforcing ONLY the epipolar constraint scores this match highly. Because the camera matrices of the two frames are available, we can obtain the ground truth fundamental matrix and thus evaluate the errors (Table 2). We can see that ASRC performs the best.

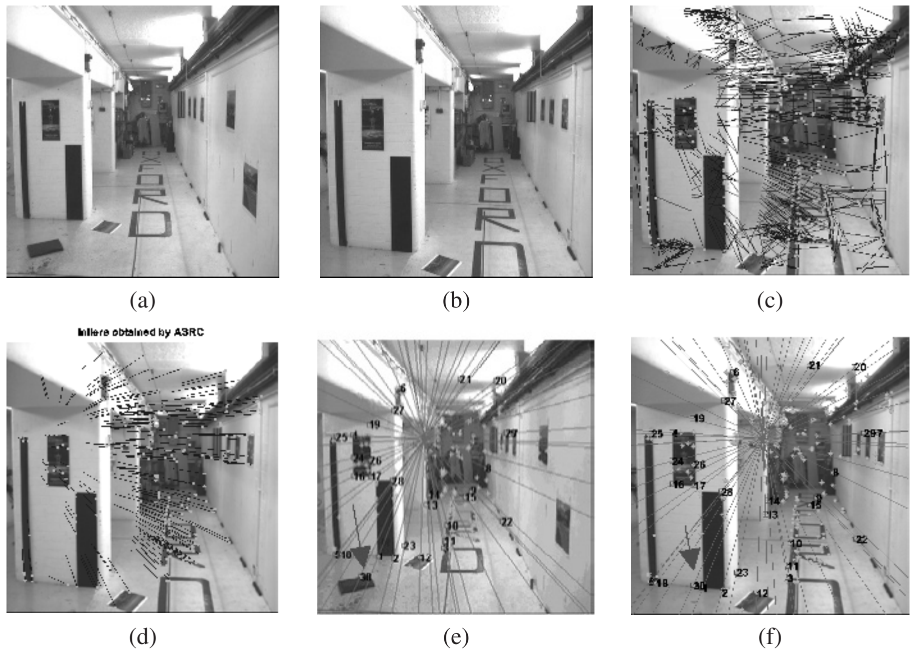

Fig. 8. (a)(b) image pair (c) matches (d) inliers by ASRC; (e)(f) epipolar geometry.

5 Conclusion

The proposed ASRC method exploits both the residuals of inliers and the corresponding scale estimate using those inliers, in determining the merit of model fit. This estimator is very robust to multiple-structural data and can tolerate more than 80% outliers The ASRC estimator is compared to those of several popular and recently proposed robust estimators: LMedS, RANSAC, MSAC, RESC, ALKS, and ASSC, showing that the ASRC estimator achieves better results (Readers may download the paper from http://www-personal.monash.edu.au/~hanzi, containing the corresponding colors figure/images, to understand the results better). Recently, a “pbM-estimator”[2], also using kernel density estimation was announced. However, this employs projection pursuit and orthogonal regression. In contrast, we consider the density distribution of the mode in the residual space.

Acknowledgements. The authors thank Andrew Zisserman, Hongdong Li, Kristy Sim, and Haifeng Chen for their valuable helps/suggestions. This work is supported by the Australia Research Council (ARC), under the grant A10017082.

References

1. Bab-Hadiashar, A., Suter, D.: *Robust Optic Flow Computation.* International Journal of Computer Vision. **29**(1) (1998) 59-77
2. Chen, H., Meer, P.: *Robust Regression with Projection Based M-estimators*. in *ICCV*. Nice, France (2003) 878-885
3. Comaniciu, D., Meer, P.: *Mean Shift Analysis and Applications.* in ICCV, Kerkyra, Greece. (1999) 1197-1203
4. Comaniciu, D., Ramesh, V., Bue, A.D.: *Multivariate Saddle Point Detection for Statistical Clustering*. in *ECCV*. Copenhagen, Danmark (2002) 561-576
5. Fischler, M.A., Rolles, R.C.: *Random Sample Consensus: A Paradigm for Model Fitting with Applications to Image Analysis and Automated Cartography.* Commun. ACM. **24**(6) (1981) 381-395
6. Haralick, R.M.: *Computer vision theory: The lack thereof.* CVGIP. **36** (1986) 372-386
7. Hoover, A., Jean-Baptiste, G., Jiang., X.: *An Experimental Comparison of Range Image Segmentation Algorithms.* IEEE Trans. PAMI. **18**(7) (1996) 673-689
8. Hough, P.V.C.: Methods and means for recognising complex patterns. U.S. Patent 3 069 654. (1962)
9. Huber, P.J.: *Robust Statistics.* New York, Wiley. (1981)
10. Lee, K.-M., Meer, P., Park, R.-H.: *Robust Adaptive Segmentation of Range Images.* IEEE Trans. PAMI. **20**(2) (1998) 200-205
11. Miller, J.V., Stewart, C.V.: *MUSE: Robust Surface Fitting Using Unbiased Scale Estimates*. in CVPR*, San Francisco* (1996) 300-306
12. Rousseeuw, P.J., Croux, C.: *Alternatives to the Median Absolute Derivation.* Journal of the American Statistical Association. **88**(424) (1993) 1273-1283
13. Rousseeuw, P.J., Leroy, A.: *Robust Regression and outlier detection.* John Wiley & Sons, New York. (1987)
14. Silverman, B.W.: *Density Estimation for Statistics and Data Analysis* London: Chapman and Hall. (1986).
15. Stewart, C.V.: *MINPRAN: A New Robust Estimator for Computer Vision.* IEEE Trans. PAMI. **17**(10) (1995) 925-938
16. Stewart, C.V.: *Bias in Robust Estimation Caused by Discontinuities and Multiple Structures.* IEEE Trans. PAMI. **19**(8) (1997) 818-833
17. Torr, P., D. Murray: *The Development and Comparison of Robust Methods for Estimating the Fundamental Matrix.* International Journal of Computer Vision. **24** (1997) 271-300
18. Torr, P., Zisserman, A.: *MLESAC: A New Robust Estimator With Application to Estimating Image Geometry.* Computer Vision and Image Understanding. **78**(1) (2000) 138-156
19. Wand, M.P., Jones, M.: *Kernel Smoothing.* Chapman & Hall. (1995)
20. Wang, H., Suter, D.: *False-Peaks-Avoiding Mean Shift Method for Unsupervised Peak-Valley Sliding Image Segmentation.* in *Digital Image Computing Techniques and Applications*. Sydney, Australia (2003) 581-590
21. Wang, H., Suter, D.: *MDPE: A Very Robust Estimator for Model Fitting and Range Image Segmentation.* International Journal of Computer Vision. (2003) to appear
22. Wang, H., Suter, D.: *Variable bandwidth QMDPE and its application in robust optic flow estimation*. in ICCV. Nice, France (2003) 178-183
23. Wang, H., Suter, D.: *Robust Adaptive-Scale Parametric Model Estimation for Computer Vision.* submitted to IEEE Trans. PAMI. (2003)
24. Yu, X., Bui, T.D., Krzyzak, A.: *Robust Estimation for Range Image Segmentation and Reconstruction.* IEEE Trans PAMI. **16**(5) (1994) 530-538
25. Zhang, Z., et al.: *A Robust Technique for Matching Two Uncalibrated Image Through the Recovery of the Unknown Epipolar Geometry.* Artificial Intelligence. **78** (1995) 87-11